

Kinetics of the Isotropic-Nematic Phase Transition in Liquid Crystals. Nucleation from Isotropic States of 4,4'-Octylcyanobiphenyl Supercooled by Shock Waves

Norbert Oranth and Frank Strohhusch*

*Institute of Physical Chemistry, University of Freiburg, Albertstrasse 21, 78 Freiburg, Germany
(Received: April 27, 1987; In Final Form: September 16, 1987)*

A metastable supercooled isotropic state of 4,4'-octylcyanobiphenyl (8CB) has been obtained by adiabatic compression of isotropic 8CB with shock waves. It transforms on a microsecond time scale to a mixture of the isotropic and nematic (n) phases, whose composition depends on the initial supercooling. The phase transition was monitored by using dielectric measurements at 30 MHz. The formation rate of the n phase is extremely dependent on the amount of supercooling, whereas the rate of its decay (after the end of the pressure pulse) is not. The results show that at low supercooling the n phase is formed by a nucleation mechanism and decays by instantaneous dissolution of the nematic droplets. Theoretical calculations using a recently developed nucleation theory of adiabatic phase transition are in good agreement with the proposed formation mechanism. Fitting the theoretical to the experimental kinetic curves allows determination of the temperature interval of metastability of the isotropic phase ΔT_c between the clearing point and the critical temperature. For 8CB a value of $\Delta T_c = 0.8$ K was found.

Introduction

The orientational order in a nematic liquid crystal breaks down at a well-defined temperature, the clearing point T_{ni} . Unlike the melting points of ordinary crystals, supercooling of the isotropic-nematic (i-n) phase transition has proved to be difficult because the formation of the nematic phase sets in with very slight supercooling, typically about 0.01 K.¹ Under conditions of microscopic observation² or DSC³ the observed transformation rates are controlled by the rate of heat flow and the temperature distribution in the probe. This shows that not only the molecular motions underlying the orientational ordering of nematogens but also the development of macroscopic order is very rapid.

Since the dynamic behavior is a matter of primary concern in liquid crystal research, we found it worthwhile to develop a new method for time-resolved observation of the thermic i-n phase transition. The basic idea consists in supercooling the isotropic phase by a sudden pressure rise. The work was done with an apparatus of the kind developed by Hoffmann and Platz⁴ and widely used for investigating reaction mechanisms in solution.⁵ It is a vertically mounted shock tube for gases with a liquid column and the measuring cell at its lower end. The conductivity measurement used so far with this technique is not suitable for studying the phase transition. Instead, we detected the change of the dielectric constant in the nonaligned liquid crystal by incorporating the measuring cell in a high-frequency impedance bridge.

In this paper the principle of the method is outlined and the experimental results obtained with 4,4'-octylcyanobiphenyl (8CB) are compared with calculations by using a recently developed nucleation theory of adiabatic phase transition.⁶ The combination of the experimental method with this theory opens a way to a detailed understanding of the formation kinetics and mechanism of the nematic phase.

Principle of the Method

The first-order transition temperature T_{ni} of nematogens increases with increasing pressure according to the Clausius-Clapeyron equation

$$\frac{dT_{ni}}{dp} = \frac{T\Delta v_{ni}}{\Delta h_{ni}} \quad (1)$$

where Δv_{ni} is the volume change and Δh_{ni} the latent heat of the n-i transition. For many nematogens the relation

$$\frac{\Delta v_{ni}}{\Delta h_{ni}} > \frac{\alpha}{C_p} \quad (2)$$

holds because of the very small value of Δh_{ni} . Here α is the thermal expansion coefficient and C_p the heat capacity of the isotropic liquid crystal. According to relation 2, the $(\partial T/\partial p)_S$ lines have smaller slopes than the phase separation line and eventually cross it.⁷ This is schematically shown in Figure 1. Starting with an isotropic sample kept at a temperature T_s slightly above T_{ni} , one can prepare supercooled states with a well-defined amount of supercooling by adiabatic compression to the appropriate final pressure p_e . A shock-wave method with controlled amplitude of the pressure step is ideal for exploring this effect.⁸

The frequency-dependent dielectric constants of 8CB have been measured as a function of temperature.⁹ At T_{ni} there is a jump from ϵ_{is} , the value in the isotropic phase, to the average $\bar{\epsilon} = (1/3)(\epsilon_{||} + 2\epsilon_{\perp})$ of the nematic phase. In Figure 2 values of the real part (ϵ') and the imaginary part (ϵ'') of ϵ_{is} and of $\bar{\epsilon}$ extrapolated from the data in ref 9 to T_{ni} are plotted over the frequency. The amplitude of the jump goes through a maximum in the relaxation range 5-50 MHz because the dispersion region of $\bar{\epsilon}$ is at smaller frequencies than that of ϵ_{is} . This behavior is typical for liquid crystals with rodlike molecules.¹⁰

When a sample is only partly transformed, the macroscopic dielectric constant ϵ takes on an intermediate value between ϵ_{is} and $\bar{\epsilon}$. Since the work of Mosotti and Clausius there have been several attempts to correlate ϵ of a macroscopically homogeneous but microscopically inhomogeneous mixture with the respective parameters of its components. Rayleigh was the first to extend the Clausius-Mosotti equation.¹¹ Bruggeman¹² and Boettcher¹³ gave different approximations for the second-order terms in the power law expansion of ϵ in terms of the electric field. Recently

(1) Kelker, H.; Hatz, R. *Handbook of Liquid Crystals*; Verlag Chemie, Weinheim, FRG, 1980; Chapter 8.5.

(2) Ostner, W.; Chan, S.-K.; Kahlweit, M. *Ber. Bunsenges. Phys. Chem.* **1973**, *77*, 1122.

(3) Armitage, D.; Price, F. P. *Mol. Cryst. Liq. Cryst.* **1978**, *44*, 33.

(4) Hoffmann, H.; Platz, G. *Ber. Bunsenges. Phys. Chem.* **1972**, *76*, 491.

(5) (a) Bernasconi, C. F. *Relaxation Kinetics*; Academic: New York, 1976. (b) Knoche, W. In *Rates and Mechanisms of Reactions*, 4th ed.; Bernasconi, C. F., Ed.; Wiley: New York, 1986.

(6) Oranth, N.; Strohhusch, F. *Ber. Bunsenges. Phys. Chem.* **1987**, *91*, 211.

(7) Horie, Y. *J. Phys. Chem. Solids* **1967**, *28*, 1569.

(8) Oranth, N. Ph.D. Dissertation, University of Freiburg, Freiburg, FRG, 1987.

(9) Buka, A.; Price, A. H. *Mol. Cryst. Liq. Cryst.* **1985**, *116*, 187.

(10) Martin, A. J.; Meier, G.; Saupe, A. *Symp. Faraday Soc.* **1971**, *5*, 119.

(11) Rayleigh, J. W. S. *Philos. Mag.* **1892**, *34*, 481.

(12) Bruggeman, D. A. G. *Ann. Phys. (Leipzig)* **1935**, *24*, 636; *Ann. Phys. (Leipzig)* **1936**, *25*, 645.

(13) Boettcher, C. J. F. *Theory of Electric Polarization*, 2th ed.; Elsevier: Amsterdam, 1973.

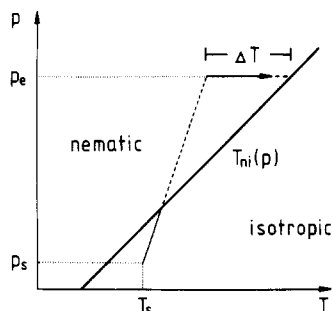


Figure 1. Phase diagram of a nematogen. Adiabatic compression starting from T_s and p_s in the isotropic phase leads to supercooling by the amount ΔT . During the transformation under constant pressure p_e the system approaches the equilibrium line.

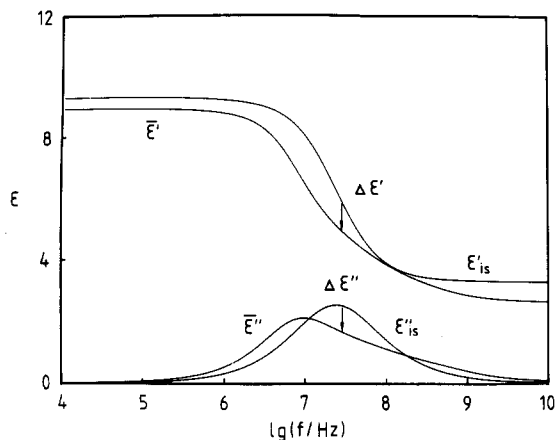


Figure 2. Frequency dependence of ϵ_{is} and $\bar{\epsilon}$ of 8CB at T_{ni} , extrapolated from the data in ref 9 (real part ϵ' , imaginary part ϵ''). The i - n phase transition results in frequency-dependent changes $\Delta\epsilon'$ and $\Delta\epsilon''$. The $\Delta\epsilon'$ and $\Delta\epsilon''$ values at 30 MHz are indicated by the arrow.

Felderhof¹⁴ used correlation integrals of the distribution to calculate upper and lower bounds for ϵ up to third order. Unfortunately, his theory involves long-range spatial correlation functions normally not known in practice. Therefore, we resort to Bruggeman's still widely used theory for ϵ of statistically distributed homogeneous spheres with different radii (permittivity ϵ_2) without interaction suspended in a medium with permittivity ϵ_1 . A change dV of the volume fraction of the spheres results in a change $d\epsilon$ given by

$$\frac{d\epsilon}{3\epsilon} = \frac{dV}{1-V} \frac{\epsilon_2 - \epsilon}{\epsilon_2 + 2\epsilon} \quad (3)$$

The growing nematic phase may be considered as consisting of homogeneous droplets. The permittivity of a single droplet can take on two different values, ϵ_{\parallel} and ϵ_{\perp} , depending on whether we are looking in the direction of the director or perpendicular to it. Thus the transformed volume may be taken as consisting of two different kinds of droplets, one-third with the permittivity ϵ_{\parallel} and two-thirds with ϵ_{\perp} . An appropriate extension of Bruggeman's theory to a suspension to the two types of nematic droplets in the isotropic mother phase is

$$\frac{d\epsilon}{3\epsilon} = \frac{dV}{1-V} \left(\frac{1}{3} \frac{\epsilon_{\parallel} - \epsilon}{\epsilon_{\parallel} + 2\epsilon} + \frac{2}{3} \frac{\epsilon_{\perp} - \epsilon}{\epsilon_{\perp} + 2\epsilon} \right) \quad (4)$$

Numerical integration of eq 4 by using ϵ_{\parallel} and ϵ_{\perp} of 8CB with the starting point ϵ_{is} results in the data shown in Figure 3 for the frequency of 30 MHz, shown together with the results of eq 3 for one kind of droplet with permittivity $\bar{\epsilon}$. We see that the correlation is nearly linear at 30 MHz. At other frequencies there are much larger differences between the different theoretical approaches. These data provide a basis for correlating ϵ in the

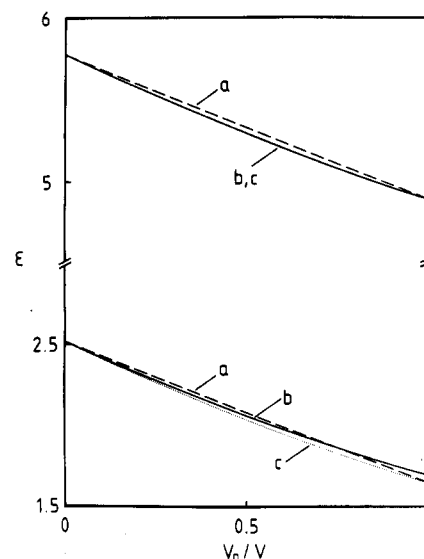


Figure 3. Permittivities at 30 MHz, ϵ' (upper curve) and ϵ'' (lower curve), of a mixture composed of spheres suspended in a homogeneous phase as a function of volume fraction of spheres: (a) linear approximation $\epsilon = \epsilon_{is} + (\bar{\epsilon} - \epsilon_{is})V_n/V$; (b) two kinds of spheres with permittivities ϵ_{\parallel} and ϵ_{\perp} , eq 4; (c) one kind of sphere with $\bar{\epsilon}$, eq 3.

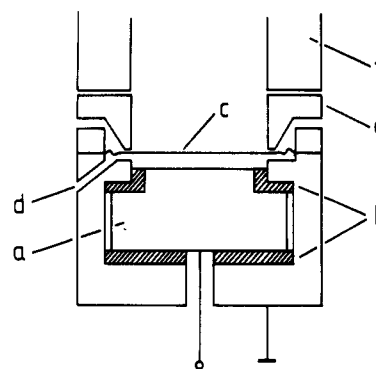


Figure 4. The measuring cell: (a) HF electrode; (b) insulation; (c) double layered foil; (d) inlet for the probe; (e) a ring which is pressed down after filling the cell, in the closed state disconnecting the inlet; (f) tube.

suspension with the degree of transformation.

Experimental Section

The high- and low-pressure sections of the thick-walled shock tube with an inner diameter of 3.5 cm have lengths of 0.8 and 2.5 m, respectively. In the lower part the gas is pressurized to 6–10 bar and in the upper part to a pressure typically between 20 and 60 bar. Bursting of the separating plastic membrane is triggered by heating two resistance wires placed directly below the membrane.¹⁵ The downward-streaming gas builds up a shock wave, which reaches the measuring cell at the end via a liquid column. The pressure is monitored in the liquid column by a piezoquartz, Kistler 601A, built into the wall of the tube 7 cm above the measuring cell. The pressure signal is digitized and stored in a transient recorder, Biomation 805. The lower part of the tube is thermostated. Its temperature is measured with a NTC sensor placed in the wall next to the measuring cell at a distance of 1 cm. The resolution of the sensor readings is ± 0.004 K and its absolute calibration ± 0.1 K. During a series of measurements of up to 8 h duration the temperature changed less than ± 0.015 K.

The measuring cell is shown in Figure 4. It is 0.5 mm high and covered with a double-layered aluminum/Hostaphan foil serving as the ground electrode. Its bottom forms the HF electrode, which is isolated against the walls with alumina. All

(14) Felderhof, B. U. *J. Phys. C* **1982**, *15*, 1731, 3943, 3953.

(15) Oranth, N.; Strobusch, F., to be published.

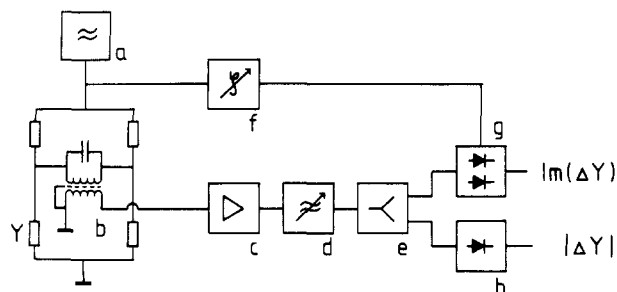


Figure 5. Detection system: (Y) cell. (a) HF generator; (b) tuner; (c) amplifier; (d) filter; (e) hybrid divider; (f) phase shifter; (g) phase-sensitive demodulator; (h) demodulator.

surfaces in contact with the liquid crystal are siliconized by treating twice with a solution of octadecyltrialkoxysilane (Aqua Sil, Pierce).¹⁶ Orientation of the liquid crystal perpendicular to the surface is thereby induced with very small anchoring energy. Because of the large dimensions of our cell, the surface effect is assumed to be negligible. The cell is filled at elevated temperature, avoiding exposure to air, through a small opening on one side.

The cell is part of the impedance bridge and detection system tuned to a carrier frequency of 30 MHz shown in Figure 5. A 0.106-V_{rms} electric field was used. The shock wave hitting the measuring cell unbalances the bridge. Its transient signal is amplified, split, and fed into two separate detection systems. In one branch a precision demodulator (S-Team; Model 664) measures the total change of admittance Y . In the other branch the imaginary part of Y is measured with a phase-sensitive detector. Both rectified signals are stored in a transient recorder, Krenz TRM 4000. The linearity of the response of the detection system was checked component by component. A detailed description is given elsewhere.⁸ The response time of the detection system was adjusted to 1 μ s, corresponding to the travel time of the shock wave through the cell.

4,4'-Octylcyanobiphenyl (8CB) from BDH was distilled at reduced pressure. $T_{ni} = 40.47$ °C.

Results and Discussion

Figure 6 shows a typical set of signals from one experiment. As the pressure transducer sits on the side of the tube, it resolves the signal into the incoming wave, the reflected wave with doubled amplitude, and the outgoing wave. At the bottom of the cell the three parts are combined to one pulse of 2/3 duration with the higher amplitude. Oscillations after each jump result from the close coupling of the pressure transducer to the liquid, since the pulse has a shorter rise time than the transducer's resonance frequency. Disturbances in the middle part arise from interactions of the reflected wave with the incoming part especially near the wall. Pressure measurements at the bottom showed that the profile there is much less disturbed. Both permittivity signals show a step with rise time equal to that of the detection system followed by a slower increase. The rapid step is present in all experiments. It is caused by the superposition of two counteracting effects: capacity increase of the cell through compression and a stronger decrease caused by a decrease of the liquid crystal permittivity under pressure. The latter is due to the increase of the relaxation time τ_{is} as pressure increases, which reduces ϵ_{is} at 30 MHz. The follow-up signal is caused by the phase transformation. It appears in those experiments where the shock-wave amplitude is sufficient to produce a state on the other side of the phase boundary. It corresponds to a decrease of ϵ , too, because $\bar{\epsilon} < \epsilon_{is}$.

Figure 7 shows a typical set of transformation signals from one series of measurements with the same initial temperature and pressure and increasing shock-wave amplitude. The bottom line shows no transformation: it is characteristic for an experiment with no or very slight supercooling. Each successive signal cor-

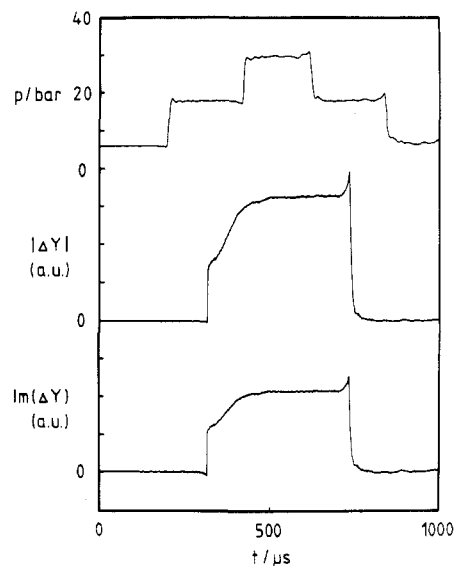


Figure 6. The signals obtained from a single shot. Starting temperature T_s , 0.11 K above T_{ni} . Upper curve: pressure as a function of time measured at the side of the shock tube; steps of the incoming wave, reflected wave, and outgoing wave. Middle curve: time dependence of the absolute value of the admittance Y of the measuring cell at the bottom of the tube. Lower curve: imaginary part of Y . The spike at the end of the pressure pulse is assumed to result from the reflection of the shock wave in the liquid at the liquid/gas interface acting as an open end.

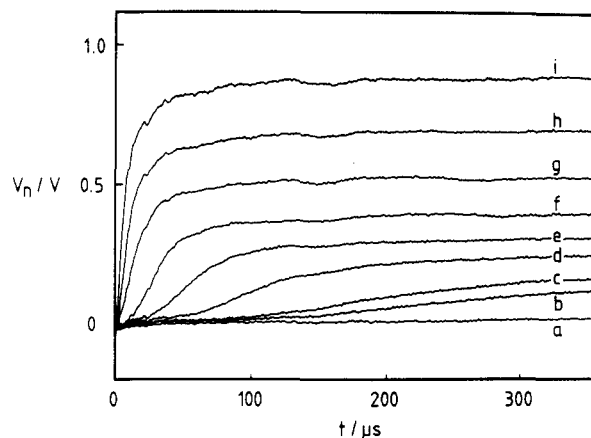


Figure 7. Transformation signal $|Y|$ as a function of the initial supercooling. Single shots. Starting parameters: $T_s = 0.11$ K above T_{ni} ; initial pressure = 6 bar. Pressure steps (bar): (a) 11.9; (b) 13.0; (c) 13.4; (d) 14.8; (e) 17.0; (f) 19.8; (g) 25.2; (h) 30.9; (i) 37.2.

responds to a greater initial supercooling, ending with a calculated 0.783 K in the top line. In most cases after a few hundred microseconds the signal does not change any more. The different amplitudes of the stationary signals reflect different degrees of transformation; i.e., in the stationary states different amounts of the isotropic and the nematic phase coexist. Now coarsening of the nematic droplets proceeds slowly without changing the macroscopic dielectric properties to a measurable extent. Theory predicts that during this slower process the temperature still rises very slightly, so that in our experiments the phase equilibrium at the temperature T_{ni} was not exactly reached.

Another important feature is the delay of the start of transformation. It decreases from about 150 μ s at 0.20 K supercooling to about 10 μ s at 0.78 K supercooling. Similar features were obtained in series of measurements with different starting temperatures and pressures.

From these results it is evident that the isotropic liquid crystal is quenched by the shock wave to a metastable state where nematic droplets must form in a thermally activated process in order to start the phase transformation. The nucleation theory of Becker and Doering¹⁷ as well as more recent theories¹⁸ predict that the

(16) (a) Perez, E.; Proust, J. E.; Ter-Minassian-Saraga, L. *Mol. Cryst. Liq. Cryst.* **1977**, *42*, 167. (b) Dubois, J. C.; Gazard, M.; Zann, A. *J. Appl. Phys.* **1976**, *47*, 1270.

TABLE I: Physical Properties of 8CB

T_{ni}/K	T^*/K	h_{ni}/J cm^{-3}	c_p/J $cm^{-3}K^{-1}$	k/J cm^{-1a}	n_o^b
313.57 ^c	312.45 ^c	2.06 ^d	2.3 ^e	2.3×10^{-14f}	6×10^{17}

^aAverage value of the elastic constants at T_{ni} . ^bNumber of correlation volumes $(4/3)\pi\xi^3$ per unit volume. The correlation length ξ at T_{ni} is given by the other parameters through $\xi = (kT_{ni}/[6h_{ni}(T_{ni} - T^*)])^{1/2}$. ^cReference 19. ^dReference 20. ^eTaken from Figure 8 in reference 20. ^fReference 21.

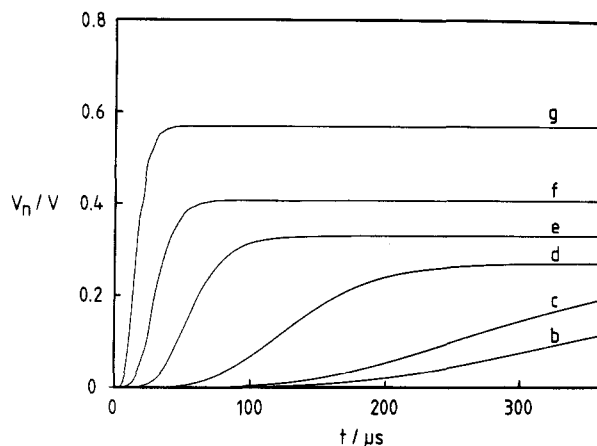


Figure 8. Calculated transformed volume fraction as a function of time for different initial supercooling (K): (b) 0.20; (c) 0.21; (d) 0.24; (e) 0.30; (f) 0.37; (g) 0.49.

formation rate of critical droplets, i.e., those with the minimum size necessary to start the transformation, is extremely temperature dependent. This explains the existence of the delay as well as its dependence upon supercooling. In a completely unstable state the transformation would onset immediately. On the other hand, the nucleation theory predicts that in an isothermal process the transformation goes to completion and that the rate increases steadily until almost all of the phase is transformed. This is in disagreement with our result that in the final state both the nematic and the isotropic phase coexist, and with the signal shape. Therefore, the adiabatic heating of the probe by the exothermic transformation must be taken into account in the treatment of the kinetics. This problem has been solved in a recently proposed nucleation theory of adiabatic processes.⁶ Here a Landau-Ginzburg equation for the growth of a single droplet was solved by using the Landau-De Gennes nematic potential function. Introducing the result into the Fokker-Planck equation of classical nucleation kinetics allows numerical integration. A detailed account of the theory is given in ref 6. The theory was used to calculate the rate of transformation from the physical properties of 8CB listed in Table I. These data are the invariant parameters governing the size- and temperature-dependent rate constants of growth and decrease of individual droplets. The free energy of formation of critical droplets $F_{dr}(R_c)$ may be considered as the parameter with analogous meaning to the activation energy in reaction kinetics. Note that $F_{dr}(R_c)$ does change with time in an adiabatic process. It was necessary to allow for this change during each experiment in order to describe our experimental results quantitatively.

As starting condition the correlation volume $(4/3)\pi\xi^3$ was taken as the individual unit in the isotropic phase, n_o being their number

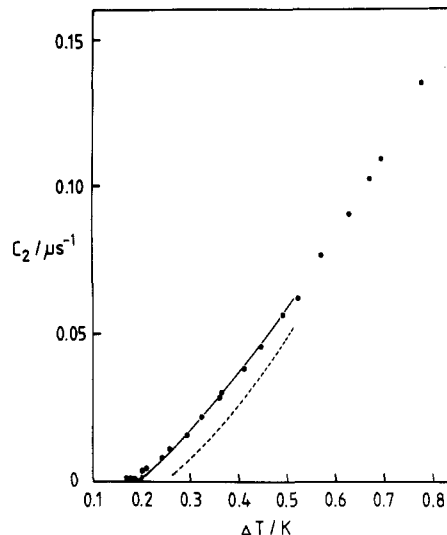


Figure 9. Plot of the rate constant c_2 against initial supercooling ΔT . Points: experiment. Dashed line: calculated with $\Delta T_c = 1.12$ K. Solid line: calculated with $\Delta T_c = 0.8$ K.

in unit volume. The numerical integration was performed in steps of time smaller than $0.4 \mu s$, and after each step the temperature change was taken into account. In Figure 8 the transformed fraction of volume is plotted as a function of time for different amounts of initial supercooling. Both the experimental and the theoretical curves may be fitted by an exponential function with three parameters c_1 - c_3 :

$$\frac{V_n}{V} = c_1 \{1 - \exp(-c_2 t)^{c_3}\}$$

In Figure 9 experimental and theoretical values of the effective rate constant c_2 are plotted against the initial supercooling ΔT . The dashed line is calculated with the literature data. Using $\Delta T_c = T_{ni} - T^* = 0.8$ K instead of the literature value 1.12 K gives the solid line. If other parameters instead of ΔT_c are changed, no substantially better fit than the dashed line is obtained.

The i - n phase transition is a first-order transition with nonpreserved order parameter. Its first-order character is reflected in the kinetics by the fact that supercooling to a metastable state is possible and that at small supercooling apparently an activation is necessary to produce the nematic droplets. Its order-disorder character is also clearly visible in the kinetics. Figure 6 shows that there is no delay in the signal decrease at the end of the pulse and that it is much faster than the increase at the beginning. After the high-pressure pulse has left the cell the pressure in the cell returns to the starting value and the initial state with a temperature higher than $T_{ni}(p_s)$ (see Figure 1) is restored. This does not happen at the same rate as the formation of the high-pressure steady state. In all our experimental observations the nematic droplets disappeared completely within a few microseconds! This clearly shows that the pressure pulses produce states far from equilibrium and that the equilibration of the latent heat between the droplets and the mother phase does not determine the kinetics. Breakdown of the nematic droplets occurs almost instantaneously, whereas their growth involving an increase of order is much slower (at least at low supercooling). At higher shock-wave pressures, when the transformation is extremely rapid, the nucleation theory is no longer applicable and one has to consider whether spinodal decomposition of the supercooled phase occurs.²²

Acknowledgment. Support of this research by the Deutsche Forschungsgemeinschaft and the Fonds der Chemischen Industrie is gratefully acknowledged.

Registry No. 8CB, 52709-84-9.

(17) Becker, R.; Döring, W. *Ann. Phys. (Leipzig)* **1935**, *24*, 719.

(18) Gunton, J. D.; San Miguel, M.; Sahni, P. S. In *Phase Transitions and Critical Phenomena*; Domb, C.; Lebowitz, J. L., Eds.; Academic: London, 1983; Vol. 8.

(19) Zink, H.; De Jeu, W. H. *Mol. Cryst. Liq. Cryst.* **1985**, *124*, 287.

(20) Thoen, J.; Murgnissen, H.; Van Dael, W. *Phys. Rev. A*, **1982**, *26*, 2886.

(21) Madhusudana, N. V.; Pratibha, R. *Mol. Cryst. Liq. Cryst.* **1982**, *89*, 249.

(22) (a) Binder, K. In *Condensed Matter Research Using Neutrons*; Lovesey, S. W.; Scherm, R., Eds.; Plenum: New York, 1984. (b) Gunton, J. D.; Droz, M. *Introduction to the Theory of Metastable and Unstable States*; Springer-Verlag: Berlin, 1983.